

文章编号: 1001-3806(2005)01-0066-02

Scattering and polarization properties of a complex refractive index spherical particle

LIU Jian-bin, WU Jian

(Department of Optoelectronic Information, University of Electronic Science & Technology of China, Chengdu 610054, China)

Abstract The scattering intensity and polarization properties of different size particles are simulated by the Riccati-Bessel functions. As the size of particles increases, the scattering intensity increases, as the size of particles increases, the horizontal polarization becomes unsymmetrical while vertical polarization invariable with the imaginary parts of complex refractive index increasing, the scattering intensity decreases. From these properties, various kinds of particles can be measured and taken apart.

Keywords scattering intensity; degree of polarization; complex refractive index; Mie's theory

球形粒子的散射和偏振特性研究

刘建斌, 吴 健

(电子科技大学 光电信息学院, 成都 610054)

摘要: 利用黎卡地-贝塞尔函数模拟了不同粒子尺度的散射光强和偏振特性。当粒子尺度增加时, 散射光强增加; 水平偏振变得不对称, 而垂直偏振没有变化; 当粒子的折射率虚部增加时, 散射光强减少。从粒子的这些散射特性和偏振特性, 可以测量和分辨不同尺度的粒子。

关键词: 散射光强; 偏振度; 复折射率; Mie理论

中图分类号: O436.3 文献标识码: A

Introduction

In recent years, theoretical treatments of scattering of spherical particles have undergone considerable progress^[1-5]. Scattering of electromagnetic waves by a spherical particle embedded in a vacuum or in a homogeneous non absorbing medium is described by Mie scattering formalism^[6,7]. The exact solution is given by an expansion in vector spherical harmonics. Several authors have attempted to generalize the Mie theory for the case of a spherical particle embedded in an absorbing medium^[8,9].

In this paper, the scattering intensity and other scattering characteristics of interest are calculated with the Riccati-Bessel functions. It is feasible to measure and distinguish from different particles.

1 Theory

The Mie scattering functions a_n and b_n are given by

$$a_n = \frac{\Psi_n(x)\Psi_n'(mx) - m\Psi_n(mx)\Psi_n'(x)}{\zeta_n(x)\Psi_n'(mx) - m\Psi_n(mx)\zeta_n'(x)} \quad (1)$$

$$b_n = \frac{m\Psi_n(x)\Psi_n'(mx) - \Psi_n(mx)\Psi_n'(x)}{m\zeta_n(x)\Psi_n'(mx) - \Psi_n(mx)\zeta_n'(x)} \quad (2)$$

Where $\Psi_n(\rho)$, $\Psi_n'(\rho)$, $\zeta_n(\rho)$ and $\zeta_n'(\rho)$ are the Riccati-Bessel functions and their derivatives with respect to the argument ρ , m is the relative complex refractive index of a particle with respect to the host medium, assuming the refractive index of the host medium is 1. The size parameter $x = 2\pi am/\lambda$, where a is the radius of the sphere, and λ is the wavelength in vacuum. The Riccati-Bessel functions are defined as $\Psi_n(\rho) = \rho J_n(\rho)$ and $\zeta_n(\rho) = \rho[(J_n(\rho) + iy_n(\rho))]$, where $J_n(\rho)$ and $y_n(\rho)$ are the n -order spherical Bessel functions of the first and the second kind. The Riccati-Bessel functions and their derivatives are evaluated at two complex arguments x and mx .

The Riccati-Bessel functions are $\Psi_n(x)$ and $X_n(x)$ are given by

$$\Psi_n(x) = \left(\frac{\pi x}{2}\right)^{1/2} J_{n+1/2}(x) \quad (3)$$

$$X_n(x) = -\frac{\pi x}{2} N_{n+1/2}(x) \quad (4)$$

基金项目: 国防科技基础研究基金资助项目 (413030305)

作者简介: 刘建斌 (1974), 男, 博士研究生, 主要从事激光大气传输特性研究。

* 通讯联系人。E-mail: wu02185@126.com

收稿日期: 2003-12-11; 收到修改稿日期: 2004-03-10

and $\zeta_n(x) = \Psi_n(x) + iX_n(x)$ (5)

Primes denote differentiation with respect to the argument

The scattered intensity of a plane electromagnetic wave of wavelength λ that is incident on a non absorbing dielectric sphere of radius a and real refractive index m is given by^[1]:

$$I = \frac{I_0 \lambda^2}{8\pi^2 r^2} (|S_1|^2 + |S_2|^2) \quad (6)$$

Where r is the distance ($r \gg \lambda$) from the sphere, I_0 is the incident intensity. The scattering functions are defined as $i_1(\theta) = |S_1(\theta)|^2$, $i_2(\theta) = |S_2(\theta)|^2$. S_1 and S_2 are the complex amplitudes function, they are defined as

$$S_1(\theta) = \sum_{n=1}^{\infty} \frac{2n+1}{n(n+1)} (\pi_n a_n + \tau_n b_n) \quad (7)$$

$$S_2(\theta) = \sum_{n=1}^{\infty} \frac{2n+1}{n(n+1)} (\tau_n a_n + \pi_n b_n) \quad (8)$$

In addition to scattering and absorption, as monochromatic electromagnetic incidents a spherical particle, it has a property called its degree of polarization. The degree of polarization is given by^[6]:

$$P = \frac{i_1(\theta) - i_2(\theta)}{i_1(\theta) + i_2(\theta)} \quad (9)$$

2 Discussion

It is interest to calculate some results obtained from the above expressions. For example, the scattering intensity of different size particles are shown in Fig. 1. The degree of polarization of different size particles is shown in Fig. 2. The relations of function between the scattering intensity and the complex refractive index are shown in Fig. 3. From these figures, we can know the scattering characteristics of a spherical particle with a laser beams incident on it. In this simulation the parameters are used $I_0 = 10^7 \text{W} \cdot \text{cm}^{-2}$; $\lambda = 1.06 \mu\text{m}$.

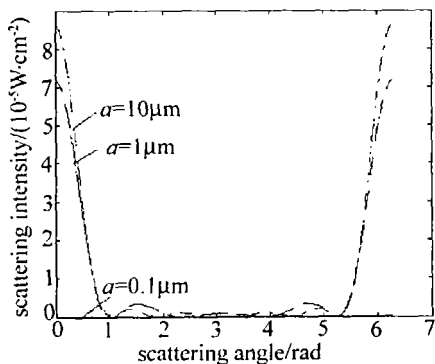


Fig. 1 Graphs of scattering intensity versus scattering angle for $a = 0.1 \mu\text{m}$, $a = 1 \mu\text{m}$, $a = 10 \mu\text{m}$, where $m = 1.33$ and $\lambda = 1.06 \mu\text{m}$

ferent size particles. As we can see from this plot with the increasing of a value, the scattering intensity increases too. Due to the particle is a sphere, the scattering intensity show high symmetry. Furthermore, the forward scattering intensity is strong while the backward scattering intensity is weak.

Fig. 2 shows the trend of degree of polarization of different size particles. It can be seen that the change of the degree of polarization is evident with the a value increasing. The horizontal polarization become unsymmetrical while vertical polarization invariable, and the value of the degree of polarization decreased.

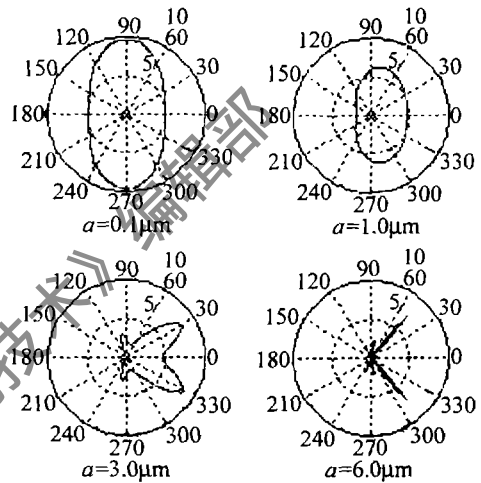


Fig. 2 Graphs of degree of polarization versus scattering angle for $a = 0.1 \mu\text{m}$, $a = 1 \mu\text{m}$, $a = 3 \mu\text{m}$, $a = 6 \mu\text{m}$, where $m = 1.33$ and $\lambda = 1.06 \mu\text{m}$

Fig. 3 shows the distribution of scattering intensity as a function of complex refractive index. As we can

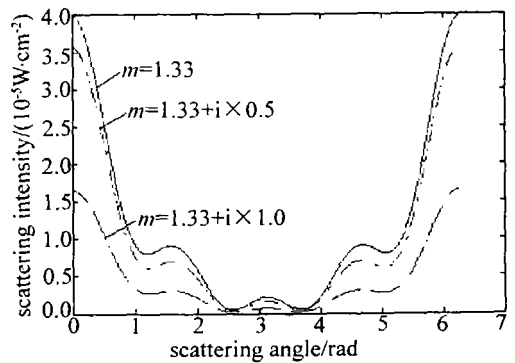


Fig. 3 Graphs of scattering intensity versus scattering angle for $m = 1.33$, $m = 1.33 + i \times 0.5$ and $m = 1.33 + i \times 1.0$ where $a = 6 \mu\text{m}$ and $\lambda = 1.06 \mu\text{m}$

see from this plot with the imaginary parts of complex refractive index increasing, the scattering intensity decreased because when the imaginary parts of complex refractive index increase, the absorption of the particles increases too. On the other hand, the scatter of the particles decreases. (下转第 112 页)

着一个初始啁啾参量的最佳值,且该值随入射功率的不同而变化。依据入射功率选择合适的初始啁啾参量

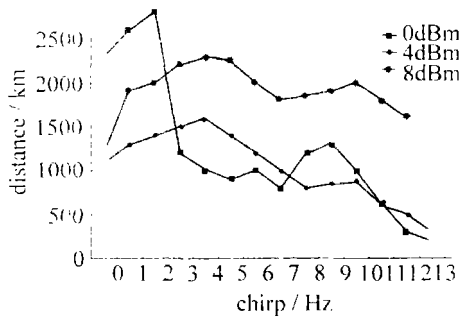


Fig 6 Function of the maximum transmission distance and pulse chirp

ing
能使传输距离大幅提升,如图6中,当脉冲平均功率为4dBm时,在 $C_0 = 3$ 处有初始啁啾脉冲传输距离近乎是无初始啁啾脉冲的2倍。但应注意到,初始啁啾也不可太大,不然会增大脉冲的相互作用,而降低系统的传输性能。

3 结论

利用初始啁啾补偿单模光纤色散效应有一定适用范围,受到一定条件限制,仅当 $C_0\beta_2 < 0$ 的条件下,线性初始啁啾对于脉冲的二阶色散(线性色散)有一定的补偿作用,而对于三阶色散,线性初始啁啾非但不能进行色散补偿,反而加剧了三阶色散对脉冲传输的不良影响。这是由于三阶色散效应所致的非线性啁啾变化是极其复杂的,不能简单地用初始线性啁啾予以补偿。在实际光纤通信系统中,要综合考虑二阶及三阶

色散效应的影响,进行合理配置,以达到最佳补偿效果。

参考文献

- [1] 李琳,蔡海文,赵玲 *et al*. 动态色散补偿技术的研究进展 [J]. 激光技术, 2002, 26(3): 194~197.
- [2] 何琼,王晶. 色散管理孤子的传输特性 [J]. 激光技术, 2002, 26(5): 367~372.
- [3] 毛幼菊,汪学强. WDM + EDFA + DCF 光纤传输系统中色散补偿方案的分析 [J]. 激光杂志, 1999, 20(6): 26~31.
- [4] HASEGAWA A. Soliton based optical communications overview [J]. Selected Topics in Quantum Electron, 2000, 6(6): 1161~1171.
- [5] 吴强,余重秀,辛雨 *et al*. $16 \times 10\text{Gbit/s}$ 啁啾光纤光栅色散补偿系统性能研究 [J]. 光子学报, 2003, 32(4): 451~453.
- [6] 刘宏展,袁明辉,曹文华. 光纤中基于互相位调制效应的超短光脉冲的产生 [J]. 光子学报, 2003, 32(6): 731~734.
- [7] 张书敏,徐文成,罗爱平 *et al*. 色散缓变光纤中飞秒光脉冲的增强压缩 [J]. 中国激光, 2001, 28(7): 599~602.
- [8] AGRAWAL G P. Effect of intrapulse stimulated Raman scattering on soliton-effect pulse compression in optical fibers [J]. Opt Lett 1990, 15(4): 224~226.
- [9] 徐文成,廖常俊,郭旗 *et al*. 色散缓变光纤对皮秒孤子的压缩效应 [J]. 光子学报, 1994, 23(3): 233~239.
- [10] 张银英,戴恩光,吴德明 *et al*. 光脉冲初始啁啾对单模光纤色散效应的影响 [J]. 光通信研究, 2002, 109(1): 41~48.
- [11] 林宁,洪小斌,张晓光 *et al*. 色散补偿技术中超短脉冲传输特性的研究 [J]. 光子学报, 1999, 28(12): 1091~1095.
- [12] 王润轩. 皮秒正啁啾脉冲的孤子效应压缩 [J]. 量子电子学报, 2003, 20(6): 741~745.
- [13] MARCUSE D, MENVUK C R. Simulation of single-channel optical systems at 100 Gbit/s [J]. J Lightwave Technol 1999, 17(4): 565~567.
- [14] MURAKAM IM, MAI M T. Long-haul $16 \times 10\text{Gbit/s}$ WDM transmission experiment using higher order fiber dispersion management technique [J]. IEEE Photon Technol Lett 1999, 11(7): 898~900.
- [15] 郭淑琴,李仲豪,肖燕 *et al*. 啁啾光脉冲在高阶色散控制光纤链中的稳定传输 [J]. 中国激光, 2001, 28(7): 645~649.
- [16] metric particles [J]. JO S A, 1991, A8(6): 871~882.
- [17] AO Ch O, KONG JA. Analytical approximations in multiple scattering of electromagnetic waves by aligned dielectric spheroids [J]. JO S A, 2002, A19(6): 1145~1156.
- [18] SKAROPOULOS N C, RUSSCHENBERG W J. Light scattering by arbitrarily oriented rotationally symmetric particles [J]. JO S A, 2002, A19(6): 1583~1591.
- [19] LOCK JA. Role of the tunneling ray in near-critical angle scattering by a dielectric sphere [J]. JO S A, 2003, A20(3): 499~507.
- [20] deHULSTH C. Light scattering by small particles [M]. New York: John Wiley & Sons, 1957, 128~130.
- [21] BOHREN C F, HUFFMAN D R. Absorption and scattering of light by small particles [M]. New York: John Wiley & Sons, 1983, 100~101.
- [22] MUNDY W C, ROUX J A, SMITH A M. Mie scattering by spheres in an absorbing medium [J]. JO S A, 1974, 64(12): 1593~1597.
- [23] CHYLEK P. Light scattering by small particles in an absorbing medium [J]. JO S A, 1977, 67(4): 561~562.

References

- [1] PROBERT-JONES J R. Resonance component of backscattering by large dielectric spheres [J]. JO S A, 1984, A1(8): 822~830.
- [2] MISHCHENKOM. Light scattering by randomly oriented axially sym-

(上接第67页)

3 Conclusion

It is very interesting to study the scattering of a spherical particle. In this simulation, the scattering intensity distribution is obtained when the size and the complex refractive index were changed. The polarization properties of different size particles were also analyzed. From these properties, it is feasible to detect and distinguish from different particles.